

ORIGINAL ARTICLE

Inhibition of farnesyl pyrophosphate synthase prevents norepinephrine–induced fibrotic responses in vascular smooth muscle cells from spontaneously hypertensive rats

Chang-Qing Du^{1,2}, Lin Yang¹, Jian Yang¹, Jie Han¹, Xiao-Sheng Hu¹, Tao Wu¹ and Shen-Jiang Hu¹

Both norepinephrine (NE) and connective tissue growth factor (CTGF) contribute to vascular fibrosis during hypertension. Recent studies indicate that farnesyl pyrophosphate synthase (FPPS) plays an important role in cardiac remodeling in hypertension. However, the role of FPPS in NE-induced fibrotic responses and related molecular mechanisms is unknown. Vascular smooth muscle cells (VSMCs) from spontaneously hypertensive rats (SHR) and Wistar-Kyoto rats (WKY) were stimulated with NE. The fibrotic responses were assessed by measuring CTGF, hydroxyproline (hyp), and α -1 procollagen I levels using Western blot, a hydroxyproline test kit, and real-time quantitative PCR assays, respectively. Ras activity was determined by a pull-down assay using a Ras activation assay kit and detected by Western blot. NE dose-dependently increased fibrosis in SHR-VSMCs, and this increase was significantly reduced by ibandronate, an inhibitor of FPPS. The addition of farnesol, but not geranylgeraniol, partially reversed the inhibitory effects of ibandronate. Furthermore, the anti-fibrotic effects of ibandronate could be mimicked by FTI-276 but not by GGTI-286. A pull-down assay showed that ibandronate reduced the NE-induced Ras activation. Moreover, ibandronate inhibited the NE-induced activation of p38, JNK, and ERK1/2. Only SB203580 (specific inhibitor of p38) diminished the NE-induced CTGF production. These results demonstrated that inhibiting FPPS prevents NE-induced fibrotic responses in SHR-VSMCs and that the Ras kinase and p38 pathways were the underlying mechanisms involved in this process. *Hypertension Research* (2014) 37, 26–34; doi:10.1038/hr.2013.96; published online 29 August 2013

Keywords: farnesyl pyrophosphate synthase; norepinephrine; vascular smooth muscle cells

INTRODUCTION

Farnesyl pyrophosphate synthase (FPPS), an essential enzyme in the mevalonate pathway, catalyzes the formation of geranyl pyrophosphate (GGPP) and farnesyl pyrophosphate (FPP) from isopentenyl pyrophosphate and dimethylallyl pyrophosphate.^{1–3} Nitrogen-containing bisphosphonates (N-BPs), such as alendronate and ibandronate, appear to act as analogues of isoprenoid diphosphate lipids, thereby inhibiting FPPS. Inhibition of this enzyme prevents the biosynthesis of isoprenoid lipids (FPP and GGPP) that are essential for the post-translational farnesylation and geranylgeranylation of small GTPase signaling proteins, which have been implicated in the pathogenesis of various cardiovascular diseases.^{1–3}

FPPS expression is significantly upregulated in several tissues (e.g., aortic smooth muscle and left ventricular) of spontaneously hypertensive rats (SHRs).^{4,5} Further studies demonstrated the increased expression of FPPS in angiotensin II (Ang II)-mediated cardiac hypertrophy both *in vitro* and *in vivo*, while inhibition or knock-down of FPPS by alendronate or RNA interference, respectively,

prevented cardiac hypertrophy.^{5,6} Moreover, chronic inhibition of FPPS by alendronate attenuates cardiac hypertrophy and fibrosis and improves endothelial function in SHRs.^{7,8} Taken together, these findings suggest that FPPS plays an important role in cardiac remodeling during hypertension. However, whether FPPS participates in vascular remodeling during hypertension remains to be determined.

Hypertension is associated with elevated sympathetic nervous system activity and increased plasma levels of catecholamines, such as epinephrine and norepinephrine (NE).⁹ NE, via α_1 -adrenoceptors (α_1 -ARs), induces vascular structural changes, including hypertrophy of the arterial wall and accumulation of extracellular matrix (ECM) proteins, and promotes the hypertrophy, hyperplasia, and proliferation of VSMCs.^{10–13} Furthermore, the potency of these effects is strongly augmented in hypertensive states.^{14,15}

Connective tissue growth factor (CTGF) is a potent profibrotic factor implicated in the hypertension-induced vascular fibrosis process.¹⁶ CTGF overexpression associated with ECM accumulation

¹Institute of Cardiology, the First Affiliated Hospital, College of Medicine, Zhejiang University, Hangzhou, P.R. China and ²Department of Cardiology, Zhejiang Hospital, Hangzhou, Zhejiang, P.R. China

Correspondence: S-J Hu, Institute of Cardiology, the First Affiliated Hospital, College of Medicine, Zhejiang University, Hangzhou 310003, P.R. China.

E-mail: s0hu0001@hotmail.com

Received 27 March 2013; revised 15 May 2013; accepted 4 June 2013; published online 29 August 2013

has been found in the aorta of SHR but not in WKY, suggesting its participation in the vascular fibrosis of SHR.¹⁷

The present study was designed to investigate whether the expression of FPPS is increased in NE-stimulated VSMCs from SHR and WKY; to determine whether ibandronate, an inhibitor of FPPS, can antagonize the NE-induced vascular fibrosis in VSMCs from SHR and WKY; and to elucidate the underlying cell signaling mechanisms of these changes, if present.

MATERIALS AND METHODS

Materials

Phosphate-buffered saline (PBS), Dulbecco's modified Eagle's medium (DMEM), penicillin-streptomycin, fetal bovine serum (FBS), and all other cell culture reagents were purchased from Gibco (Life Technologies, MO, USA). Farnesol (FOH) and geranylgeraniol (GGOH) were purchased in soluble form. The MAPK inhibitors used in the present study were PD-98059 (ERK1/2 inhibitor), SB-203580 (p38 MAPK inhibitor), and SP-600125 (JNK1, JNK2, and JNK3 inhibitor). The inhibitors were dissolved in DMSO at 10 mM (final concentration of DMSO in medium was 1:1000, v/v). Unless otherwise noted, the rest of the agents for cell treatment were prepared in sterile saline and diluted in DMEM to the working concentration. Stock solutions of NE-HCl were freshly prepared in water on the day of the experiment. Phospho-ERK1/2 (p-ERK1/2), ERK1/2, phospho-p38 (p-p38), p38, and anti-rabbit horseradish peroxidase (HRP)-conjugated IgG were obtained from Cell Signaling Technology (Danvers, MA). Phospho-JNK1/2/3 (p-JNK1/2/3) and JNK1 antibodies were obtained from Epitomics (Burlingame, CA, USA). Goat anti-CTGF polyclonal antibody was obtained from Santa Cruz Biotechnology (Santa Cruz, CA, USA). Enhanced chemiluminescence (ECL) reagent was from Amersham International (Bucks, UK). The Ras activation assay kit was purchased from Cytoskeleton, Inc. (S. Acoma St, Denver, USA). Unless otherwise specified, the drugs used were purchased from Sigma (St Louis, MO, USA).

Experimental animals

Specific pathogen-free male SHR and normotensive Wistar-Kyoto (WKY) rats, 10 weeks of age, were obtained from the Experimental Animal Center, Chinese Academy of Sciences (Shanghai, China). Systolic blood pressure (SBP) was recorded in conscious rats using the tail-cuff method. The SBP was significantly higher ($P < 0.001$) in SHR (180 ± 3.5 mm Hg) than in WKY rats (114 ± 2.8 mm Hg). The animals were housed in a room with a constant climate and a 12-h light/dark cycle and were provided with free water and a 20% (W/W) protein commercial chow. All procedures were performed in accordance with the revised 1996 National Institutes of Health guidelines for the care and use of laboratory animals (NIH Publication No. 85-23) and the Animal Care Committee of Zhejiang University, Zhejiang province, China.

Smooth muscle cell culture and treatment

VSMCs were obtained from the thoracic aortas of 10-week-old male WKY and SHR using the collagenase method, as previously described.¹⁸ Cells between passages 3 and 5 were used in all experiments. Quiescence was established by transferring cells to six-well culture plates at 80% confluence, followed by two incubations: the first for 24 h in DMEM containing 10% FBS and the second for 48 h in DMEM containing 0.1% FBS. The cell cultures were incubated in a humidified incubator at 37 °C and 5% CO₂ in the presence or absence of NE at different concentrations (0.01, 0.1, 1, and 10 μM) for 24 h. In some experiments, the cells were preincubated for 2 h with 10 μM ibandronate (Iban), Iban plus GGOH (30 μM), Iban plus FOH (30 μM), GGTI-286 (selective inhibitor of GGTase I, 10 μM), or FTI-276 (selective inhibitor of farnesyltransferase, 10 μM). To inhibit the MAPK pathway, PD98059 (ERK1/2 inhibitor, 50 μM), SB203580 (p38 MAPK inhibitor, 10 μM), and SP600125 (JNK-1,-2,-3 inhibitor, 10 μM) were added 2 h before the stimulus in some experiments. None of the inhibitors were toxic at the doses used, and none had an effect on the basal CTGF levels. The respective solvent control did not affect any of the parameters measured.

Cell proliferation assay

The effect of Iban on NE-stimulated VSMC proliferation was determined using a Cell Counting Kit (CCK-8) (Dojindo laboratory, Japan) according to the manufacturer's protocol. Briefly, cells were grown in 96-well plates at a density of 1×10^4 per well. After the indicated treatments, 10 μl CCK-8 solution was added to each well, which was incubated at 37 °C for an additional 2 h. Absorbance at 450 nm was measured using a Bio-Rad 680 microplate reader (USA). The results of the CCK-8 assay are nearly proportional to the cell number and can thus be used to determine the proliferation and cytotoxicity. The cell proliferation is expressed as the optical density.

Cell apoptosis assay

VSMC apoptosis was detected using the Annexin V-FITC Apoptosis detection kit (BioVision) according to the manufacturer's protocol. Briefly, after incubation with Iban of different concentrations for 24 h, both floating and attached cells were harvested and washed twice with PBS. Isolated VSMCs (1×10^6 cells/ml) were resuspended in 500 μl of binding buffer. A FITC-annexin V (5 μl) and propidium iodide (PI, 5 μl) working solution was added, and then the cells were incubated at room temperature for 5 min in the dark. After the incubation period, the cells were analyzed using flow cytometry (FACS Calibur, USA), the annexin V-FITC binding was analyzed using a FITC signal detector (FL1), and PI staining was measured by a phycoerythrin emission signal detector (FL3). Apoptotic cells were identified as annexin V (+) and PI (-).

Total RNA preparation and real-time quantitative polymerase chain reaction analysis (RT-qPCR)

The mRNA expression levels of CTGF, FPPS, α -1 procollagen I, and the reference gene glyceraldehyde-3-phosphate dehydrogenase (GAPDH) were analyzed by real-time quantitative polymerase chain reaction analysis (RT-qPCR). Total RNA was isolated from treated VSMCs using a Trizol kit (Invitrogen Life Technologies) according to the manufacturer's instructions. RT-qPCR was performed on an ABI PRISM 7000 sequence detection system (Applied Biosystems, Foster City, CA) with the SYBR Green PCR master mix (Applied Biosystems). The primer sequences for each gene (Sangon, Shanghai, China) are listed as follows: CTGF forward, 5'-CAGGGAGTAAGGGAC ACGA-3'; reverse, 5'-ACAGCAGTTAGGAACCCAGAT-3'; FPPS forward, 5'-TGAAGTGGATGAACTGGGACA-3'; reverse, 5'-GAGGAAGAAAGCCTG GAGCA-3'; α -1 procollagen I forward, 5'-GAGCCTAACCATCTGGCATCT-3'; reverse, 5'-AGAACGAGGTAGTCTTTTCAGCAAC-3'; and GAPDH forward, 5'-GGAAAGCTGTGGCGTGAT-3'; reverse, 5'-AAGGTGGAAGAATGGGAG TT-3'. Data were analyzed with Sequence Detection System software (Applied Biosystems). The relative expression CTGF, FPPS, pro-collagen I mRNA was normalized to that of GAPDH mRNA to obtain a normalized target value. Each of the experimental normalized sample values was divided by one normalized control sample value (calibrator) to generate the relative expression level.

Western blotting

The CTGF protein and the ERK1/2, p38, and JNK phosphorylation levels in total protein extracts were determined by Western blot. Cells were treated as described above and then washed with PBS and lysed in lysis buffer. The protein concentration was determined using the BCA method. Equal amounts of protein (30 μg) were denatured and loaded onto a 10% sodium dodecyl sulfate-polyacrylamide gel electrophoresis (SDS-PAGE) followed by Western Blot analysis using primary antibodies (CTGF, phospho-ERK, total ERK, phospho-p38 MAPK, total p38 MAPK, phospho-JNK, JNK, (all at a 1:1000 dilution)) and then incubated for 16–18 h at 4 °C. Membranes were washed three times with TBST for 10 min and then incubated with horseradish peroxidase-conjugated anti-goat (1:8000 dilution) or goat anti-rabbit IgG antibody (1:2000 dilution) for 1 h at room temperature. After incubation with the secondary antibody, the membranes were rinsed three times with TBST for 10 min, and the antigen-antibody complex was detected using an ECL Plus system (Amersham Bioscience, Piscataway, NJ, USA). To ensure equal protein loading, GAPDH was used as an endogenous control. The results are expressed

as the n-fold increase over controls in densitometric arbitrary units using the mean \pm s.e.m. of the data.

Hydroxyproline content assay

Hydroxyproline (Hyp) levels (as an index of collagen) in the culture supernatant were measured in duplicate using colorimetric methods according to the hydroxyproline test kit instructions (Institute of Jiancheng Bioengineering, Nanjing, China). Briefly, at the end of culture, the medium was aspirated from each well and centrifuged (500 g, 5 min) to remove the cell debris. One milliliter of supernatant fluid was used to determine the Hyp content with the Hyp standard at 550 nm wavelengths. The collagen level was calculated from

the product of the Hyp content (micrograms per milligram of protein, $\mu\text{g}/\text{mg}$ prot) according to the formulae given in the instructions.

Ras activation assay

The activation state of Ras was measured with a pull-down assay according to the instructions in the Ras Activation Assay Kit (Cytoskeleton, BK008, Denver, CO, USA). In brief, 80% confluent VSMCs in 10 cm tissue culture plates were serum starved for 48 h before the addition of Iban ($10 \mu\text{M}$) for 24 h, followed by stimulation with or without norepinephrine ($0.1 \mu\text{M}$) for 30 min and processing. Ras-GTP from the cell lysates ($50 \mu\text{g}$ per point quantified by Bradford) was 'pulled down' with Raf1-RBD (Ras binding domain) beads and detected

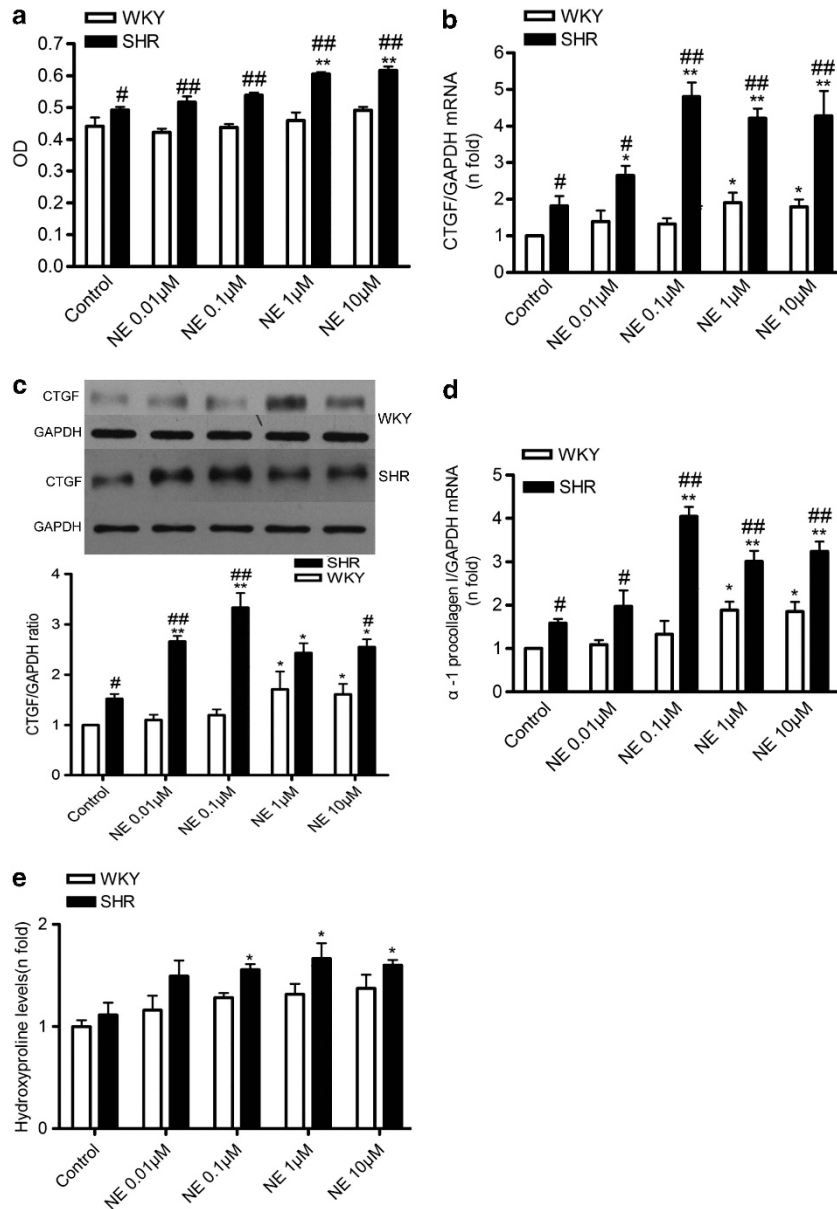


Figure 1 NE exerts greater effects on proliferation, CTGF and ECM upregulation in cultured VSMCs from SHR than WKY. Quiescent VSMCs from SHR and WKY were incubated with NE (0.01, 0.1, 1, $10 \mu\text{M}$) for 24 h. (a) shows cell proliferation expressed as the optical density which was determined by Cell Counting Kit (CCK-8). (b) shows levels of CTGF mRNAs as determined by RT-qPCR analysis. The ratio of CTGF mRNAs is set to '1' for WKY control group. (c) shows in top panel a representative western blot of CTGF protein expression and in bottom data bar chart. The ratio of CTGF protein is set to '1' for WKY control group. (d) shows levels of type I pro-collagen mRNAs as determined by RT-qPCR analysis. The ratio of α -1 procollagen I mRNAs is set to '1' for WKY control group. (e) shows Hydroxyproline (Hyp) levels (as an index of collagen) in the culture supernatant as measured with the Hyp test kit. The level of hydroxyproline is set to '1' for WKY control group. Data are expressed as mean \pm s.e.m. ($n=5$). # $P<0.05$, ## $P<0.01$ vs corresponding WKY group; * $P<0.05$, ** $P<0.01$ vs corresponding control group.

by 12% SDS-PAGE and Western blotting using anti-Ras antibody. For comparison with the Ras activity (level of GTP-bound Ras) in the same samples, 20 µg of total cell lysate per sample was used to detect the total amount of Ras in the supernatant. In addition, GAPDH protein was used as the internal control.

Statistical analysis

The results are presented as the mean ± s.e.m. Data sets containing multiple groups were evaluated using one-way ANOVA, followed by the *post hoc* least-significant difference test with the SPSS 15.0 program (SPSS Inc., Chicago, IL), after an *F* test for the homogeneity of variances had been performed. If the data failed to meet the requirements for equal variance, a Tamhane T2 test was used. The results were considered statistically significant at a value of $P < 0.05$. The normotensive WKY group was used as the calibrator with a given value of 1, and the other groups were compared with this calibrator.

RESULTS

Effect of NE on proliferation, CTGF and ECM upregulation in cultured VSMCs from SHR and WKY

SHR-VSMCs exhibited greater proliferation in the presence or absence of NE than did WKY-VSMCs (Figure 1a). NE (0.01, 0.1, 1, and 10 µM) treatment for 24 h markedly increased the proliferation of SHR-VSMCs in a concentration-dependent manner, with the maximal response at 1 µM ($P < 0.01$); the NE treatment slightly stimulated the proliferation of WKY-VSMCs ($P > 0.05$).

The baseline mRNA and protein levels of CTGF were higher in SHR-VSMCs than in WKY-VSMCs. NE treatment significantly increased the mRNA and protein levels of CTGF in SHR-VSMCs relative to those in the WKY-VSMCs receiving the same dose of treatment (Figures 1b and c). The maximal response in SHR-SMCs was observed with 0.1 µM NE (Figures 1b and c). In addition, NE increased the expression of different ECM-related proteins, including the gene expression of α -1 procollagen I and the Hyp content in the conditioned medium (Figures 1d and e). The NE-induced increases in ECM-related protein synthesis in SHR-VSMCs were also significantly greater than those in WKY-VSMCs.

Induction of FPPS by NE in VSMCs

SHR-VSMCs and WKY-VSMCs spontaneously expressed FPPS at the mRNA and protein levels. The SHR-VSMCs exhibited enhanced baseline FPPS expression compared with that in WKY-VSMCs (Figure 2a). Incubation with NE (0.01, 0.1, 1, and 10 µM) for 24 h increased the FPPS mRNA expression at 0.01 µM in a dose-dependent manner in SHR-VSMCs and only at 1 µM in WKY-VSMCs. Meanwhile, the protein expression of FPPS was elevated significantly for 0.01 µM NE in SHR-VSMCs, with maximal responses at 10 µM. The NE treatment increased the protein expression of FPPS only at 1 µM in WKY-VSMCs. All of the above results suggest that FPPS expression could be more easily elicited by NE in SHR-VSMCs.

Ibandronate decreases the proliferation, Hyp content, and CTGF protein expression elicited by NE in cultured VSMCs from SHR

To investigate the potential role of FPPS in the vascular fibrosis elicited by NE, the ant-fibrotic effects of an FPPS inhibitor, ibandronate, were tested in NE-induced fibrosis in SHR-VSMCs.

First, the effects of ibandronate on cell proliferation were studied. Preincubation with ibandronate (5, 10 µM) for 2 h reduced the NE-induced cell proliferation in SHR-VSMCs in a dose-dependent manner (Figure 3A). However, ibandronate alone did not influence the cell proliferation in either strain. Similarly, the NE-mediated

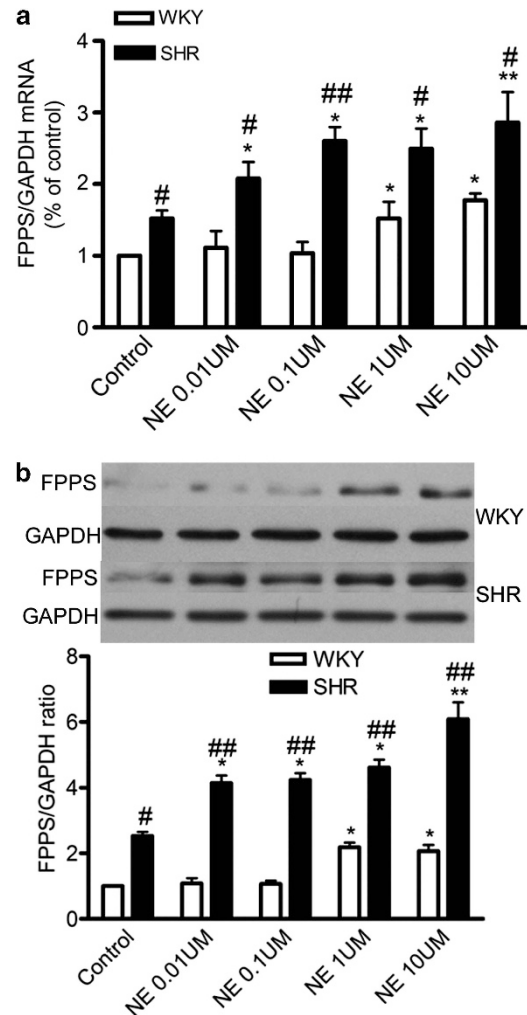


Figure 2 Expression of FPPS mRNAs (a) and protein (b) in VSMCs from WKY and SHR before and after NE treatment. Quiescent VSMCs from SHR and WKY were incubated with NE (0.01, 0.1, 1, 10 µM) for 24 h. Levels of FPPS mRNAs and protein were determined by RT-qPCR analysis, Western blot respectively. The ratio of FPPS mRNAs (a) and protein (b) is set to '1' for WKY control group. Data are expressed as mean ± s.e.m. ($n = 5$). [#] $P < 0.05$, ^{**} $P < 0.01$ vs corresponding WKY group; ^{*} $P < 0.05$, ^{**} $P < 0.01$ vs corresponding control group.

induction of Hyp in SHR-VSMCs was markedly reduced in the presence of ibandronate, whereas ibandronate alone had no effect on the Hyp levels (Figure 3B). Consistent with our results for collagen deposition, the ability of NE to induce CTGF protein expression in SHR-SMCs was reduced in the presence of ibandronate (Figure 3C), whereas ibandronate alone had no effect on the CTGF protein expression (Figure 3C). The addition of ibandronate alone did not reduce the CTGF protein expression or Hyp levels below the basal levels observed in the controls, indicating that ibandronate suppressed the profibrotic effect of excess NE while leaving the basal levels unaltered. To further verify that the antifibrotic effect of ibandronate *in vitro* was not due to an apoptotic effect in VSMCs, we investigated the influence of ibandronate on cell apoptosis in SHR-VSMCs. The results shown in Figure 3D demonstrated that ibandronate exerted no effect on cell apoptosis in SHR-VSMCs. Collectively, these results suggest that ibandronate reversed the ability of NE to induce vascular fibrosis in SHR-VSMCs.

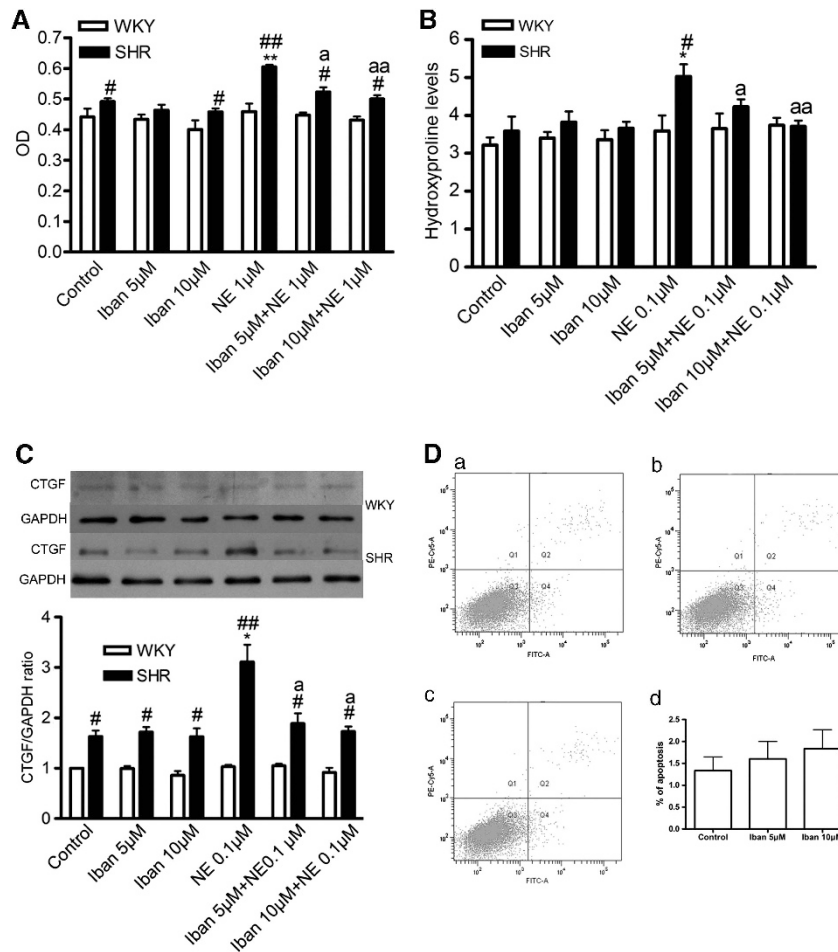


Figure 3 Ibandronate decreases proliferation, CTGF protein expression, Hyp upregulation elicited by NE in cultured VSMCs from SHR. **(A)** Quiescent VSMCs from both strains were pre-incubated with ibandronate (5, 10 μ M) for 2 h and then incubated with or without NE (1 μ M) for 24 h. Cell proliferation was expressed as the optical density which was determined by Cell Counting Kit (CCK-8). **(B)** Quiescent VSMCs from both strains were pre-incubated with ibandronate (5, 10 μ M) for 2 h and then incubated with or without NE (0.1 μ M) for 24 h. Hydroxyproline (Hyp) levels (as an index of collagen) in the culture supernatant were measured by the Hyp test kit. **(C)** Quiescent VSMCs from both strains were pre-incubated with ibandronate (5, 10 μ M) for 2 h and then incubated with or without NE (0.1 μ M) for 24 h. Levels of CTGF protein was determined by Western blot. The ratio of CTGF is set to '1' for WKY control group. **(D)** Effects of ibandronate on the apoptosis of SHR-VSMCs. Incubation of quiescent SHR-VSMCs with ibandronate in a series of final concentrations (0, 5, and 10 μ M) for 24 h induced no apoptosis. Representative diagrams altered by different concentrations of Ibandronate are shown: (a) control, (b) treatment with 5 μ M of ibandronate, (c) treatment with 10 μ M of ibandronate, (d) representative bar chart showing percentage of apoptotic cells. Data are expressed as mean \pm s.e.m. ($n=5$). [#] $P<0.05$, ^{##} $P<0.01$ vs corresponding WKY group; ^{*} $P<0.05$, ^{**} $P<0.01$ vs corresponding control group. ^a $P<0.05$, ^{aa} $P<0.01$ vs NE treated SHR-VSMC group. A full color version of this figure is available at the *Hypertension Research* journal online.

The effect of ibandronate is mediated through the inhibition of farnesylated proteins

CTGF is a vascular fibrosis mediator implicated in the hypertension-induced pathologic vascular fibrosis process and has been suggested to be a useful molecular marker of the fibrotic response.^{18–20} To investigate the molecular mechanism of the ibandronate-mediated inhibition of NE-induced vascular fibrosis, we investigated the effects of FOH or GGOH on CTGF regulation. FOH, but not GGOH, partly reversed the inhibitory action of ibandronate on the induction of CTGF (Figure 4), suggesting that farnesylated proteins, and therefore Ras signaling, may participate in CTGF regulation, whereas geranylgeranylated proteins are not involved. The importance of the isoprenylation of Ras proteins for CTGF induction was further established using FTI-276, an inhibitor of farnesyltransferase. Pretreatment of the SHR-VSMCs with FTI-276 for 2 h substantially reduced the NE-mediated induction of CTGF, while GGTI-286, an

inhibitor of the geranylgeranyltransferase-I, did not show any significant effects (Figure 4).

Ibandronate modulates NE-induced Ras activation in cultured SHR-VSMCs

We next evaluated whether ibandronate could inhibit the NE-induced activation of the small G protein Ras. Stimulation with NE (0.1 μ M) for 30 min increased the GTP-bound Ras levels, as shown by pull-down assays, which were diminished by pretreatment with 10 μ M ibandronate for 24 h (Figure 5). These data demonstrate that ibandronate inhibits the NE-induced Ras activation.

Ibandronate diminishes NE-induced MAPK activation in cultured SHR-VSMCs

To further investigate the molecular mechanism underlying the ability of ibandronate to suppress the NE induction of CTGF, the

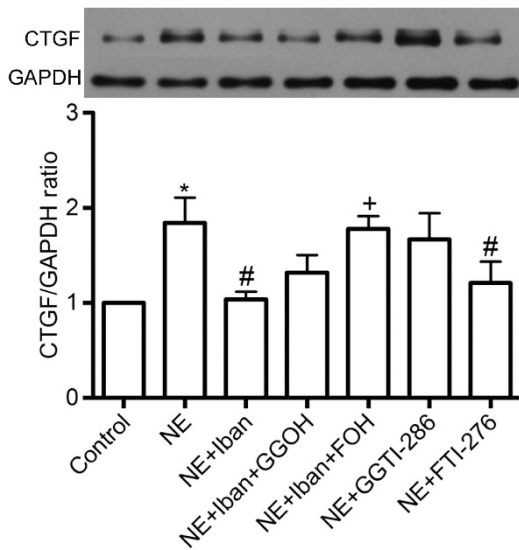


Figure 4 The ant-fibrotic effect of ibandronate is mediated through the inhibition of farnesylated proteins. Quiescent VSMCs from SHR were pre-incubated with ibandronate (10 μ M), GGTI-286 (10 μ M) or FTI-276 (10 μ M) for 2 h and then incubated with or without NE (0.1 μ M) for 24 h. Some cells were also incubated with GGOH (30 μ M), FOH (30 μ M) 1 h before the addition of the Iban. Results of total CTGF production were obtained from densitometric analysis and expressed as ratio CTGF/GAPDH as n-fold over control. Figure shows in top panel a representative Western blot and in bottom data total CTGF production as means \pm s.e.m. of 3 independent experiments. The ratio of CTGF is set to '1' for SHR control group. * P <0.05 vs control, # P <0.05 vs NE, + P <0.05 vs NE + Iban.

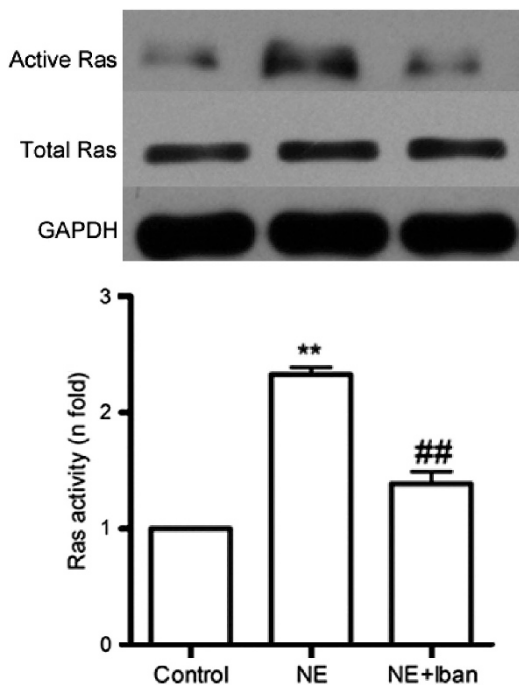


Figure 5 Ibandronate diminishes Ras activation in NE-treated SHR-VSMCs. Cells were pretreated for 24 h with Iban 10 μ M and then stimulated with NE 0.1 μ M for 30 min. Ras activity was determined by pull down assays. Figure shows in top panel a representative Western blot and in bottom as means \pm s.e.m. of 3 independent experiments. As loading control Ras and GAPDH expression levels were evaluated in total cell lysates. The ratio of active Ras is set to '1' for SHR control group. ** P <0.01 vs control, ## P <0.01 vs NE.

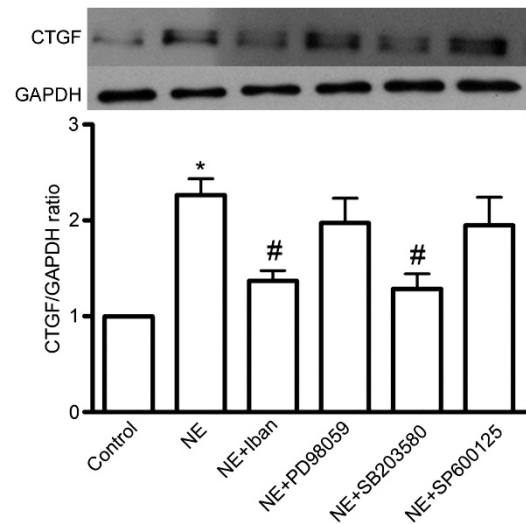


Figure 6 Inhibition of p38MAPK diminishes NE-induced CTGF production. SHR-VSMCs were preincubated for 2 h with 10 μ M Iban (FPPS inhibitor), 10 μ M SB203580 (p38 inhibitor), 50 μ M PD98059 (ERK-p42/44 inhibitor) or 10 μ M SP600125 (JNK inhibitor) before treatment with 0.1 μ M NE for 24 h. Figure shows in top panel a representative Western blot and in bottom data total CTGF production as means \pm s.e.m. of 3 independent experiments. The ratio of CTGF is set to '1' for SHR control group. * P <0.01 vs control, # P <0.01 vs NE.

involvement of the MAPK cascade in the CTGF regulation by NE was evaluated using specific inhibitors of the p38 MAPK (SB203580), extracellular signal-regulated kinase (ERK) 1/2 (PD98059), and Jun N-terminal kinase (JNK) (SP600125) cascades. Only p38 inhibitors diminished the NE-induced CTGF production (Figure 6). These data show that NE upregulates CTGF via activation of p38 MAPK in SHR-VSMCs.

NE is known to induce ERK, JNK, and p38 phosphorylation in VSMCs.²¹⁻²³ We next evaluated whether ibandronate could inhibit the NE-induced activation of these pathways. In SHR-VSMCs, NE (0.1 μ M, 5 min) treatment triggered phosphorylation of all three MAPKs. Preincubation with ibandronate inhibited the NE-induced activation of p38, JNK, and ERK1/2 (Figure 7), suggesting that inhibition of p38 could be involved in the CTGF downregulation by ibandronate.

DISCUSSION

The present study showed for the first time that FPPS is overexpressed and easily elicited by NE in aortic SHR-VSMCs compared with WKY-VSMCs. Furthermore, the NE-induced fibrotic responses were greater in SHR-VSMCs. Ibandronate, a FPPS inhibitor, can inhibit the NE-induced fibrotic reaction in SHR-VSMCs. The underlying mechanism involves inhibition of Ras signaling and modulation of the p38 MAPK pathway. Thus, FPPS could be involved in vascular fibrosis in the setting of hypertension.

Multiple studies demonstrated that FPPS is inhibited by N-BPs; this inhibition in turn prevents prenylation of small GTPases, including Ras, and regulates several processes in various diseases. N-BPs have been used to treat bone and cancer diseases by inhibiting the activation of Ras through the suppression of both farnesylation and geranylgeranylation.^{24,25} Ras proteins are expressed in almost all types of cells, including fibroblasts and muscle cells,²⁶ and activate signal transduction pathways that regulate cellular proliferation, differentiation, and survival.²⁷ Farnesylation of Ras by

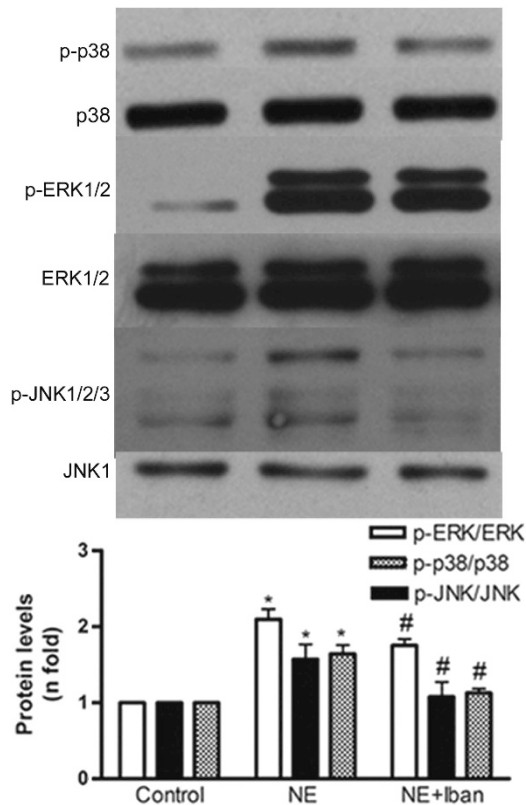


Figure 7 Ibandronate diminishes MAPK activation in NE-treated SHR-VSMCs. Cells were pretreated for 24 h with Iban ($10\mu\text{M}$), and then stimulated with $0.1\mu\text{M}$ NE for 5 min. Figure shows a representative Western blot of phospho-p38 (p-p38), phospho-ERK (p-ERK1/2) and phospho-JNK (p-JNK1/2/3) and p38, ERK and JNK (used as controls). Figures show data as mean \pm s.e.m. of 3 experiments. The ratio of p-ERK1/2 or p-p38 or p-JNK1/2/3 is set to '1' for SHR control group. * $P < 0.05$ vs control. # $P < 0.05$ vs NE.

farnesyltransferase (FTase) is required for the proper membrane localization and activity of Ras.²⁷ Farnesyl thiosalicylic acid (FTS), a Ras antagonist, attenuated fibrosis and improved muscle strength in a dy/dy mouse model of congenital muscular dystrophy.²⁸ Furthermore, in an earlier study, FPP, but not GGPP, was found to completely restore the anti-angiogenic effects of incadronate disodium on advanced glycation end product (AGE)-exposed endothelial cells.²¹

Vascular fibrosis is one of the main features of hypertension.²² The exaggerated proliferation and excessive accumulation of ECM proteins induced by NE in VSMCs contribute to this pathophysiological process.^{10–13,22} α_1 -ARs are G-coupled receptors that activate several intracellular signaling systems, including the Ras/mitogen-activated protein kinase (MAPK) pathway and the redox process, which regulate several NE-mediated responses.^{11,29,30} Blockage of α_1 -AR-mediated smooth muscle cell hypertrophy by inhibitors of 3-hydroxy 3-methylglutaryl coenzyme A reductase has been observed, which suggests the involvement of farnesol, a derivative of mevalonate metabolites.³¹ In this study, the ibandronate-induced inhibition of NE-induced vascular fibrosis was restored by FOH but not by GGOH, suggesting that the anti-fibrotic effect of ibandronate may be associated, at least in part, with the suppression of FPP and thus might occur via limitation of Ras farnesylation (Figure 4). The importance of the isoprenylation of Ras proteins for the NE-induced CTGF production was further

substantiated by the data shown in Figure 5. Thus, these results suggest that inhibition of Ras activation is important for the protective effects of ibandronate against NE-induced fibrotic responses in SHR-VSMCs.

The MAPK family of serine/threonine-specific protein kinases consists of three isoforms: ERK, p38, and JNK.²³ A growing body of evidence suggests that ERK1/2,³² p38,³³ and JNK³⁴ are activated by NE in VSMCs. These activated MAPKs are involved in NE-induced vascular structural and functional changes.^{10–13} In SHR-VSMCs, NE treatment triggered phosphorylation of all three MAPKs (Figure 7). Inhibition of FPPS diminished the phosphorylation of ERK1/2, JNK, and p38 in response to NE, which suggests that FPPS might affect the activation of ERK1/2, JNK and p38 MAPK by NE in SHR-VSMCs. However, only p38 inhibitors diminished the NE-induced CTGF production (Figure 6). These data indicated that p38 MAPK could be involved in the ibandronate-mediated inhibition of NE-induced vascular fibrosis in SHR-VSMCs.

p38 MAPK has been suggested to be an important regulator of vascular fibrosis in SHR, while the ERK1/2, PI3K/Akt, and JNK MAPK pathways play a major role in vascular hyperplasia and hypertrophy.^{35,36} The importance of p38 MAPK in vascular fibrosis was further supported by a study showing that p38 MAPK inhibitors diminished Ang II-induced CTGF production in VSMCs.¹⁸ All these data indicated that p38 MAPK is an important regulator of vascular fibrosis in the setting of hypertension. Thus, we conclude that the inhibitory effect of ibandronate on NE-induced CTGF production in SHR-VSMCs could be involved in preventing the activation of p38 MAPK.

In the present study, NE treatment was found to stimulate the proliferation of cultured SHR-VSMCs while showing no proliferative effect on WKY-VSMCs. Our data are consistent with a previous study showing that NE stimulation of Wistar aortic SMCs significantly increases protein synthesis while not inducing cell proliferation.¹²

It has been suggested that activation of the Ras/Raf-1/ERK1/2 MAPK pathway is required for NE-stimulated VSMC proliferation.^{29,37} This cascade is also implicated in cell proliferation in many other types of cells.^{38,39} Ras mediates its effects on cellular proliferation in part by activation of a cascade of kinases: Raf (c-Raf-1, A-Raf, and B-Raf), MEK (MAPK/ERK kinases 1 and 2), and ERK1/2.^{29,38} Ras activates this kinase cascade by directly binding to Raf, which requires active, GTP-bound Ras and an intact effector domain. Ibandronate prevents NE-induced Ras activation and cell proliferation in SHR-VSMCs. This finding suggested that ibandronate may exert its cellular proliferative inhibitory effects through suppression of the Ras/Raf-1/ERK1/2 MAPK pathway elicited by NE in SHR-VSMCs.

It is generally accepted that Ras plays a central role in signal transduction pathways that respond to diverse extracellular stimuli, including peptide growth factors, cytokines, and hormones. Increasing evidence has indicated that the events downstream of Ras are more complex than simply activating Raf kinase. Ras was reported to activate three distinct MAPK cascades (ERK, JNK, and p38) through Raf-1 or MEKs.⁴⁰ Raf causes direct activation of ERK but not JNK/p38,^{40,41} whereas MEKs activate JNK/p38 but not ERK.⁴⁰ The small G protein Ras has also been shown to play a key role in the activation of p38 MAPK by multiple stimuli, including hemopoietic cytokines, platelet-derived growth factor, IL-1, and fibroblast growth factor.^{42–45} The interaction between Ras activation and p38 MAPK in the SHR-VSMCs in response to NE requires further investigation.

The evidence reported in this study as well as that from the literature indicate a possible role of FPPS in the pathogenesis of

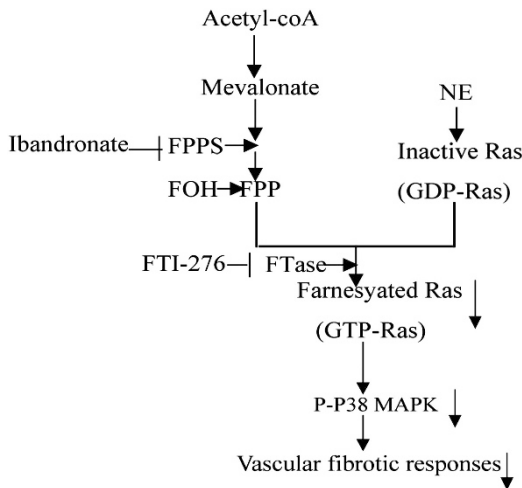


Figure 8 Summary of the novel signaling mechanisms underlying regulation of FPPS in NE-induced fibrotic responses in SHR-VSMCs. Inhibition of FPPS prevents NE-induced fibrotic responses via regulation of Ras and P38 MAPK activation in SHR-VSMCs. Theoretically, inhibition of FPPS could inhibit the NE-induced fibrotic reaction in the setting of hypertension.

vascular and cardiac remodeling in SHR rats. Indeed, previous studies demonstrated that inhibition or knockdown of FPPS by alendronate or RNA interference, respectively, prevented cardiac hypertrophy and fibrosis in SHRs.^{6,7} In addition, cardiac-specific overexpression of FPPS has recently been demonstrated to induce cardiac hypertrophy and heart failure in mice, suggesting that FPPS may function as a potent regulator in myocardial remodeling.⁴⁶ However, the above studies did not focus on the *in vivo* role of FPPS in vascular remodeling. Furthermore, although bisphosphonates have been shown to have inhibitory effects on the development of experimental atherosclerosis and neointimal hyperplasia in animal models,⁴⁷ whether the possible inhibitory effects depend on the mevalonate pathway and FPPS remains unclear. The present finding, in which FPPS inhibition prevents NE-induced fibrotic responses in SHR-VSMCs, may lead to novel targeted therapies for hypertensive vascular diseases. However, although the most powerful nitrogen-containing BPs (such as alendronate, ibandronate, and zoledronate) can inhibit the mevalonate pathway and FPPS in particular, these BPs are commonly used in clinical practice to treat osteoporosis by inhibiting osteoclastic activity and bone resorption. In view of the above facts, a series *in vivo* experiments focusing on the following aspects are needed to validate the critical role of FPPS in vascular remodeling: a) the knockout of the FPPS gene in hypertensive animals, b) the use of antisense oligonucleotides against FPPS, or c) the design of new, highly selective FPPS antagonists.

CONCLUSION

The present study demonstrates for the first time that the upregulation of FPPS expression triggered by NE may be involved in vascular remodeling in the setting of hypertension (Figure 8). Promising areas for future research include the knockout of the FPPS gene in hypertensive animals, the use of antisense oligonucleotides against this enzyme, and the design of new, highly selective FPPS antagonists with therapeutic potential.

CONFLICT OF INTEREST

The authors declare no conflict of interest.

ACKNOWLEDGEMENTS

This work was supported by the National Natural Sciences Foundation of China (project numbers 30470715, 30870939), the Research Fund for the Doctoral Program of Higher Education of China (No. 20040335118), Zhejiang Provincial Natural Science Foundation of China (Grant No. Y2080374), and the National Natural Sciences Foundation of China (Project for Young Scientists, No. 30800999).

- Roskoski Jr R. Protein prenylation: a pivotal posttranslational process. *Biochem Biophys Res Commun* 2003; **303**: 1–7.
- Casey PJ. Protein lipidation in cell signaling. *Science* 1995; **268**: 221–225.
- Szkopin' ska A, Plochocka D. Farnesyl diphosphate synthase: regulation of product specificity. *Acta Biochim Pol* 2005; **52**: 45–55.
- Li L, Hu SJ, Dong HT, Kang L, Chen NY, Fang YQ. Alterations in gene expression of series key enzymes in mevalonic acid pathway detected by RNA array in spontaneously hypertensive rats. *Chin J Pathophysiol* 2008; **24**: 54–59.
- Ye Y, Hu SJ, Li L. Inhibition of farnesylpyrophosphate synthase prevents angiotensin II-induced hypertrophic responses in rat neonatal cardiomyocytes: involvement of the RhoA/Rho kinase pathway. *FEBS Lett* 2009; **583**: 2997–3003.
- Ye Y, Mou Y, Bai B, Li L, Chen GP, Hu SJ. Knockdown of farnesyl pyrophosphate synthase prevents angiotensin II-mediated cardiac hypertrophy. *Int J Biochem Cell Biol* 2010; **42**: 2056–2064.
- Li L, Chen GP, Yang Y, Ye Y, Yao L, Hu SJ. Chronic inhibition of farnesyl pyrophosphate synthase attenuates cardiac hypertrophy and fibrosis in spontaneously hypertensive rats. *Biochem Pharmacol* 2010; **79**: 399–406.
- Chen GP, Li L, Yang Y, Fu M, Yao L, Wu T, Zhang XQ, Hu SJ. Chronic inhibition of farnesyl pyrophosphate synthase improves endothelial function in spontaneously hypertensive rats. *Biochem Pharmacol* 2010; **80**: 1684–1689.
- Julius S, Majahalme S. The changing face of sympathetic overactivity in hypertension. *Ann Med* 2000; **32**: 365–370.
- Hu ZW, Shi XY, Lin RZ, Hoffman BB. α 1 adrenergic receptors activate phosphatidylinositol 3-kinase in human vascular smooth muscle cells. Role in mitogenesis. *J Biol Chem* 1996; **271**: 8977–8982.
- Xin X, Yang N, Eckhart AD, Faber JE. α 1D-adrenergic receptors and mitogen-activated protein kinase mediate increased protein synthesis by arterial smooth muscle. *Mol Pharmacol* 1997; **51**: 764–775.
- Chen L, Xin X, Eckhart AD, Yang N, Faber JE. Regulation of vascular smooth muscle growth by alpha 1-adrenoreceptor subtypes in vitro and in situ. *J Biol Chem* 1995; **270**: 30980–30988.
- Yu SM, Tsai SY, Guh JH, Ko FN, Teng CM, Ou JT. Mechanism of catecholamine-induced proliferation of vascular smooth muscle cells. *Circulation* 1996; **94**: 547–554.
- Ibarra M, López-Guerrero JJ, Villalobos-Molina R. Further evidence for the predominance of α 1D-adrenoceptors in arteries of normotensive and spontaneously hypertensive rats. *Pharmacol Rev Commun* 1998; **10**: 135–142.
- Villalobos-Molina R, Ibarra M. Increased expression and function of vascular alpha1D-adrenoceptors may mediate the prohypertensive effects of angiotensin II. *Mol Interv* 2005; **5**: 340–342.
- Perbal B. CCN proteins: multifunctional signalling regulators. *Lancet* 2004; **363**: 62–64.
- de las Heras N, Ruiz-Ortega M, Rupérez M, Sanz-Rosa D, Miana M, Aragoncillo P, Mezzano S, Lahera V, Egido J, Cachofeiro V. Role of connective tissue growth factor in vascular and renal damage associated with hypertension in rats. Interactions with angiotensin II. *J Renin Angiotensin Aldosterone Syst* 2006; **7**: 192–200.
- Rupérez M, Lorenzo O, Blanco-Colio LM, Esteban V, Egido J, Ruiz-Ortega M. The connective tissue growth factor is a mediator of angiotensin II-induced fibrosis. *Circulation* 2003; **108**: 1499–1505.
- Verrecchia F, Mauviel A. Transforming growth factor-beta signaling through the Smad pathway: role in extracellular matrix gene expression and regulation. *J Invest Dermatol* 2002; **118**: 211–215.
- Leask A, Holmes SA, Shiwen X, Black CM, Abraham DJ. The control of ccn2 (ctgf) gene expression in normal and scleroderma fibroblasts. *Mol Petrol* 2001; **54**: 180–183.
- Okamoto T, Yamagishi S, Inagaki Y, Amano S, Takeuchi M, Kikuchi S, Ohno S, Yoshimura A. Incadronate disodium inhibits advanced glycation end products-induced angiogenesis in vitro. *Biochem Biophys Res Commun* 2002; **297**: 419–424.
- Tunon J, Ruiz-Ortega M, Egido J. Regulation of matrix proteins and impact on vascular structure. *Curr Hypertens Rep* 2000; **2**: 106–113.
- Miyata Y, Nishida E. Distantly related cousins of MAP kinase: biochemical properties and possible physiological functions. *Biochem Biophys Res Commun* 1999; **266**: 291–295.
- Jagdev SP, Coleman RE, Shipman CM, Rostami HA, Croucher PI. The bisphosphonate, zoledronic acid, induces apoptosis of breast cancer cells: evidence for synergy with paclitaxel. *Br J Cancer* 2001; **84**: 1126–1134.
- Berenson J, Ravera C, Ma P, Deckert F, Sasaki Y, Saeki T, Takahima S, LoRusso P, Goodin S, Seaman J, Schran H, Zhou H. Population pharmacokinetics of zometax. (Abstract) Proc Am Soc Clin Oncol 2000; **19**: 209(a).

- 26 Marom M, Haklai R, Ben-Baruch G, Marciano D, Egozi Y, Kloog Y. Selective inhibition of Ras-dependent cell growth by farnesylthiosalicylic acid. *J Biol Chem* 1995; **270**: 22263–22270.
- 27 Reuther GW, Der CJ. The Ras branch of small GTPases: Ras family members don't fall far from the tree. *Curr Opin Cell Biol* 2000; **12**: 157–165.
- 28 Nevo Y, Aga-Mizrachi S, Elmakayes E, Yanay N, Ettinger K, Elbaz M, Brunschwig Z, Dadush O, Elad-Sfadia G, Haklai R, Kloog Y, Chapman J, Reif S. The Ras antagonist, farnesylthiosalicylic acid (FTS), decreases fibrosis and improves muscle strength in *dy* mouse model of muscular dystrophy. *PLoS One* 2011; **6**: e18049.
- 29 Muthalif MM, Uddin MR, Fatima S, Parmentier JH, Khandekar Z, Malik KU. Small GTP binding protein Ras contributes to norepinephrine induced mitogenesis of vascular smooth muscle cells. *Prostaglandins Other Lipid Mediat* 2001; **65**: 33–43.
- 30 Bleeke T, Zhang H, Madamanchi H, Patterson C, Faber JE. Catecholamine-induced vascular wall growth is dependent on generation of reactive oxygen species. *Circulation Res* 2004; **94**: 37–45.
- 31 Nishio E, Kanda Y, Watanabe Y. α 1-Adrenoceptor stimulation causes vascular smooth muscle cell hypertrophy: a possible role for isoprenoid intermediates. *Eur J Pharmacol* 1998; **347**: 125.
- 32 Dessy C, Kim I, Sougnéz CL, Laporte R, Morgan KG. A role for MAP kinase in differentiated smooth muscle contraction evoked by α -adrenoceptor stimulation. *Am J Physiol* 1998; **275**: C1081–C1086.
- 33 Kalyankrishna S, Malik KU. Norepinephrine-induced stimulation of p38 mitogen-activated protein kinase is mediated by arachidonic acid metabolites generated by activation of cytosolic phospholipase A (2) in vascular smooth muscle cells. *J Pharmacol Exp Ther* 2003; **304**: 761–772.
- 34 Lee YR, Lee CK, Park HJ, Kim H, Kim J, Kim J, Lee KS, Lee YL, Min KO, Kim B. c-Jun N-terminal kinase contributes to norepinephrine-induced contraction through phosphorylation of caldesmon in rat aortic smooth muscle. *J Pharmacol Sci* 2006; **100**: 119–125.
- 35 Touyz RM, He G, El Mabrouk M, Schiffrin EL. p38 Map kinase regulates vascular smooth muscle cell collagen synthesis by angiotensin II in SHR but not in WKY. *Hypertension* 2001; **37**: 574–580.
- 36 El Mabrouk M, Touyz RM, Schiffrin EL. Differential ANG II-induced growth activation pathways in mesenteric artery smooth muscle cells from SHR. *Am J Physiol Heart Circ Physiol* 2001; **281**: H30–H39.
- 37 Egan SE, Weinberg RA. The pathway to signal achievement. *Nature* 1993; **365**: 781–783.
- 38 Tanaka K, Abe M, Sato Y. Roles of extracellular signal-regulated kinase1/2 and p38 mitogen-activated protein kinase in the signal transduction of basic fibroblast growth factor in endothelial cells during angiogenesis. *Jpn J Cancer Res* 1999; **90**: 647–654.
- 39 Talarmin H, Rescan C, Cariou S, Glaise D, Zanninelli G, Bilodeau M, Loyer P, Guguen-Guillouzo C, Baffet G. The mitogen-activated protein kinase kinase/extracellular signal-regulated kinase cascade activation is a key signalling pathway involved in the regulation of G (1) phase progression in proliferating hepatocytes. *Mol Cell Biol* 1999; **19**: 6003–6011.
- 40 Minden A, Lin A, McMahon M, Lange-Carter C, Derijard B, Davis RJ, Johnson GL, Karin M. Differential activation of ERK and JNK mitogen-activated protein kinases by Raf-1 and MEKK. *Science* 1994; **266**: 1719–1723.
- 41 Olson MF, Ashworth A, Hall A. An essential role for Rho, Rac, and Cdc42 GTPases in cell cycle progression through G1. *Science* 1995; **269**: 1270–1272.
- 42 Tan Y, Rouse J, Zhang A, Cariati S, Cohen P, Comb MJ. FGF and stress regulate CREB and ATF-1 via a pathway involving p38 MAP kinase and MAPKAP kinase-2. *EMBO J* 1996; **15**: 4629–4642.
- 43 Rausch O, Marshall CJ. Cooperation of p38 and extracellular signal-regulated kinase mitogen-activated protein kinase pathways during granulocyte colony-stimulating factor-induced hemopoietic cell proliferation. *J Biol Chem* 1999; **274**: 4096–4105.
- 44 Palsson EM, Popoff M, Thelestam M, O'Neill LA. Divergent roles for Ras and Rap in the activation of p38 mitogen-activated protein kinase by interleukin-1. *J Biol Chem* 2000; **275**: 7818–7825.
- 45 Li C, Hu Y, Sturm G, Wick G, Xu Q. Ras/Rac-Dependent activation of p38 mitogen-activated protein kinases in smooth muscle cells stimulated by cyclic strain stress. *Arterioscler Thromb Vasc Biol* 2000; **20**: E1–E9.
- 46 Yang J, Mou Y, Wu T, Ye Y, Jiang JC, Zhao CZ, Zhu HH, Du CQ, Zhou L, Hu SJ. Cardiac-specific overexpression of farnesyl pyrophosphate synthase induces cardiac hypertrophy and dysfunction in mice. *Cardiovasc Res* 2013; **97**: 490–499.
- 47 Wu L, Zhu L, Shi WH, Yu B, Cai D. Zoledronate inhibits intimal hyperplasia in balloon-injured rat carotid artery. *Eur J Vasc Endovasc Surg* 2011; **41**: 288–293.